Applications of Densiometry, Ultrasonic Speed Measurements, and Ultralow Shear Viscosimetry to Aqueous Fluids

Gerhard Fritz, Günther Scherf, and Otto Glatter*

Chemistry Department, University of Graz, Heinrichstrasse 28, A-8010 Graz, Austria

Received: September 13, 1999; In Final Form: January 21, 2000

Precision measurements of density and sound velocity can be used to follow changes in fluids such as micellization or phase separation. Both techniques have been implemented in the oscillating tube density meters in different sample cells for several years. However, to get better results for the density of viscous samples, a correction for viscosity effects is necessary. Therefore, a viscosity-dependent signal must be measured, which can be achieved by determining the damping of the oscillating tube. This is done routinely in the latest generation of such density meters. We present a method to convert this measured signal into actual viscosity data up to about 300 mPa·s and show some applications of all three measured signals to different problems in the field of the study of complex fluids: Density and sound velocity can be used to establish water or any other pure fluid as a secondary standard for small angle scattering experiments. Viscosity shows temperature-dependent structural changes and the critical temperature of diblock copolymers of the C_iE_j type. Finally, all three parameters—density, sound velocity, and viscosity—are used to establish a phase diagram of the PEO−PPO−PEO triblock copolymer P94 in aqueous solution.

Introduction

Methods such as densiometry, ultrasonic speed measurements, and viscosimetry are common and easily performed techniques that offer valuable contributions to the interpretation of the phase behavior of liquids.[1,2,3] Also, they are, in many cases, additional tools to more sophisticated methods and may be, in some cases, essential for the interpretation of other measurements, such as the specific volume, which can be determined from density, for the calculation of molecular weight using SAXS,[4,5] or the viscosity, necessary for the determination of size distributions using DLS.

One instrument family that is widely used to perform such experiments are the DMA densiometers (Anton Paar KG, Graz, Austria), which use the oscillating-tube technique. These instruments can be equipped with an additional ultrasonic speed measurement cell.[6] However, just within the last few years, a measurement mode using the oscillating tube has been developed to compensate viscosity effects that may lead to certain errors in the density measurements.[7] The signal that is obtained from this measurement mode and used for the calculation of the corrected density is consequently a function of the viscosity. In this paper, we present an easy and stable technique to convert this signal into viscosity values.

Application of such a DMA to the determination of phase diagrams seems to be promising, especially for complex fluids. Because of the three measurement parameters, which are determined independently, a wide range of different phase boundaries can be detected. The observed changes may even give the first hints as to the nature of the corresponding phases and what might happen at the phase boundary. Additionally, the absolute values of the measured parameters can be used in many ways, such as the calculation of compressibility or the specific volume.

* To whom correspondence should be addressed. E-mail: otto.glatter@kfunigraz.ac.at. Fax: +43/316/380 9850.

A small contact area to air at the filling holes, which can be sealed easily, and the excellent thermostatisation of the sample cells allow the investigation of volatile and sensible samples. If the samples are measured with the temperature being changed automatically, the increase or decrease is performed in a stepwise mode. This allows, contrary to a DSC, very slow temperature variations, or even time-dependent measurements at constant temperature.[8]

To demonstrate the capabilities of the DMA, we show examples of water and aqueous solutions of nonionic surfactants of the C_iE_j type[9] and the PEO−PPO−PEO type.[10,11,12,13]

Experimental Section

Materials. The calibration silicone oil W46 C2124 has been supported by S & H Kalibrier und Prüftechnik (DKD-K-10 701), Graz, Austria. Poly(ethylene glycol) alkyl ether diblock copolymers C_iE_j, by Bachem, Germany (C_8E_3, C_8E_4, C_8E_5, $C_{10}E_4$) and Fluka, Switzerland ($C_{12}E_4$, $C_{12}E_5$, $C_{12}E_6$), have been made available by Reinhard Strey. The ICI PEO−PPO−PEO triblock copolymer P94 has been obtained from Erbslöh, Germany and used without further purification.

All of the concentrations are given in % (w/w).

Experimental. The dynamic capillary rheometric measurements have been done using a Dynamic Capillary Rheometer (Anton Paar KG, Graz) with a 100 mm long capillary of 3 mm diameter, at a frequency of 1 Hz.

Most of the measurements have been performed using three prototypes of the DMA 5000 (Anton Paar KG, Graz), which have been modified by the addition of ultrasonic sound cells equivalent to DSA 48 (Anton Paar KG, Graz). The necessary sample volumes are about 1.5 mL for the density/viscosity cell and 0.7 mL for the sound velocity cell. The thermostatisation of the instrument is correct to 10 mK in absolute values.

First, the measurements have been controlled using a C++ Program by the Labor für Messtechnik, Graz, and later using a

10.1021/jp993237u CCC: $19.00
Published on Web 03/28/2000

Fortran 90 Windows program that has been developed in our group. This Fortran program has also been used for data evaluation. The measurements can be performed automatically in a time-dependent manner, with a time resolution of about 1 min, or with temperature steps as small as to 10 mK. The typical parameters for each measurement point of temperature-dependent investigations are thermostatisation for 5 min and multiple measurements over a period of 10 min.

Densiometry and Ultralow Shear Viscosimetry. The well-established oscillating-tube technique for density measurements determines the oscillation frequency of a U-shaped borsilica-glass tube filled with the sample.[14,15] The tube is about 2×75 mm, and its diameter is 2 mm. Good temperature control of the tube is essential because an inaccuracy of 40 mK can lead to a density difference of up to 10^{-4} g/mL. It is also crucial to ensure a constant temperature along the whole length of the tube. Both tasks can be achieved by coupling the tube to a thermostated block of copper by means of a hydrogen atmosphere to ensure good thermal conductivity. The temperatures of both, the hydrogen near the oscillating tube the copper, are measured to improve the temperature control. Another experimental detail that can lead to serious problems for some densities is the parasitic resonance of other components, such as the electronic parts. These effects can be minimized by strongly linking the measuring cell to the 8 kg countermass, which is connected to the housing by elastic supports. This setup acts like a mechanical filter for external oscillations. The countermass has a resonance frequency of 100 Hz, which is far below the frequencies used for density measurements. The heavy countermass also ensures that the two nodal points of the tube are in a nearly constant position, regardless of the mass filled into the tube, thereby minimizing nonlinearity effects. Another possible source of nonlinearity is a nonuniform mass distribution along the oscillator, as would be the case if an excitation magnet is used at the end of the tube. Therefore, the oscillation frequency is measured by means of the modulation of an infrared light beam reflected by a thin layer of gold at the end of the tube.

The sample volume is set by the two nodal points, where the tube is fixed to the wall and the frequency depends only on the mass of the sample and tube and the spring constant of the tube. An external force, by means of a piezo element, compensates the damping of the whole system. Parameters that correspond to the sample volume and the spring constant can be determined by means of two calibration measurements (usually water and air), allowing the calculation of the actual sample density with an accuracy of about 1×10^{-6} g/mL for samples of low viscosity.

To avoid any memory effects of the glass tube after temperature changes, all of the frequencies are measured relative to a built-in reference oscillator. Nevertheless, samples of high viscosity give rise to problems for cases in which this simple experimental setup is used: The liquid in the tube does not only perform the translatorial movement in the vertical direction during the oscillation, but it also moves with rotational components. This rotational contribution is damped by the viscosity of the fluid, which leads to an apparent mass that is higher than the true one, which yields a deviation of up to 0.8×10^{-3} g/mL for the measured density. To correct for these effects, a parameter that is related to the viscosity must be determined.

To avoid the necessity of an additional apparatus, a method has been developed to measure this parameter by means of the external force.[7,16,17] Normally, this force is used in a phase mode that compensates only for the damping, to ensure that a quasi-harmonic oscillation is observed. But the external force can be applied in a phase-shifted mode as well. In this case, it must be secured that damping is still compensated, but a contribution of the force slightly affects the oscillation frequency.[18] This contribution has a fixed relation to the amount of damping. The ratio of the periods in the normal oscillation mode, P_O, and the phase-shifted mode, P_{OS}, allow the calculation of a loss-angle ratio, Tg_O

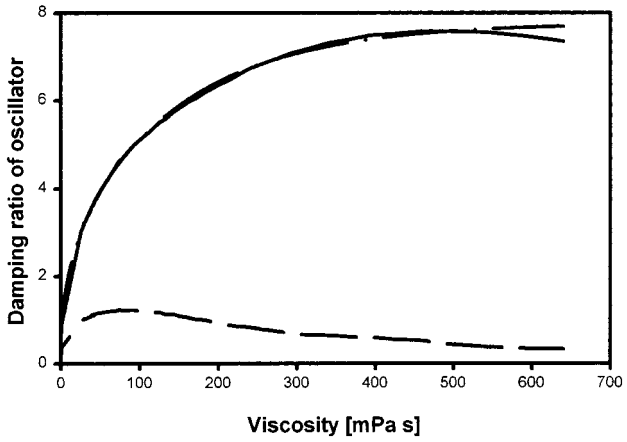

Figure 1. The damping ratio of the oscillator in the fundamental (dashed line) and the first harmonic mode (solid line). The fit, used for viscosity calculation, is the dashed−dotted curve.

$$Tg_O = \left[\left(\frac{P_O}{P_{OS}}\right)^2 - 1\right] \cdot \frac{P_{OS}}{8 \cdot R_{CO} \cdot \pi \cdot 10^2} \qquad (1)$$

where R_{CO} is a constant that depends on the instrument. The effects of the temperature history are excluded by referring to the loss-angle ratio of the reference oscillator Tg_R

$$D_O = Tg_O - Tg_R \qquad (2)$$

Finally, only the damping of the sample is of interest, whereas the contribution of the glass tube can be eliminated by subtracting the damping of the tube filled with air, which has a sufficiently low viscosity

$$\Delta D_O = D_O - D_{OAir} \qquad (3)$$

These damping values increase with increasing viscosity for liquids with low viscosities but reach a maximum value at about 80 mPa·s (Figure 1). Further increase in viscosity leads to a steady decrease of the measured signal. To shift the maximum to higher values and get a better signal, the damping measurements are not done in the fundamental but in the first harmonic oscillation, which shifts the maximum and, therefore, the upper limit of the usable viscosity regime to about 500 mPa·s.

The density, ρ, can be calculated from the fundamental periods of the tube, P_F, and the reference oscillator, P_R, with the viscosity effects taken into account by

$$\rho = A \cdot (1 + V_1 \cdot \Delta D_O + V_2 \cdot \Delta D_O^2) \cdot \left(\frac{P_F}{P_R}\right)^2 - B \qquad (4)$$

where V_1 and V_2 are calibration parameters that can be determined by measuring viscous density calibration oils (Normally the factory settings $V_1 = 0$ and $V_2 = -8 \times 10^{-6}$ are sufficient). A and B correspond to the spring constant and the sample volume in the tube,respectively, and can be calculated

from

$$A = \frac{\rho_{water} - \rho_{air}}{\left(\frac{P_{Fwater}}{P_R}\right)^2 \cdot (1 + V_1 \cdot \Delta D_{Owater} + V_2 \cdot \Delta D_{Owater}^2) - \left(\frac{P_{Fair}}{P_R}\right)^2}$$

$$B = A \cdot \left(\frac{P_{Fair}}{P_R}\right)^2 - \rho_{air} \quad (5)$$

The damping data are not only necessary for the correction of the density, but viscosity itself can be derived from them. To convert between the two parameters, a continuous function that calculates the damping from the viscosity, η, must be established. The function

$$\Delta D_O = y_0 + A_1 \cdot (1 - e^{-\eta/f_1}) + A_2 \cdot (1 - e^{-\eta/f_2}) + A_3 \cdot (1 - e^{-\eta/f_3}) \quad (6)$$

gives good fits to the experimental data from $\eta = 0$ up to the maximum damping, η_{max}, but to avoid possible problems concerning a nonlinear least-squares calculation, one can fix the values for f_1, f_2, and f_3 to 5, 25, and 150, respectively, which gives reasonable results. Equation 6 cannot be transformed to give η directly because of its transcendental nature, but using this approximation, viscosities can be calculated for a given damping value by means of the regula falsi from $\eta = 0$ to η_{max}.

Damping values near the maximum, at about 500 mPa·s, would lead to badly determined viscosities and must be excluded from evaluation. Nevertheless, ambiguity remains for damping values corresponding to viscosities that are lower and higher than η_{max}. This ambiguity can be eliminated by calculating the ratio between the damping values obtained in the first harmonic and fundamental oscillation modes. If this ratio is lower than the empirical coefficient, 10.0, then the viscosity is lower than 500 mPa·s, which allows the exclusion of viscosities from 500 mPa·s to at least 2500 mPa·s.

The determination of the viscosity calibration curve is accomplished by measuring samples of known viscosities: The two measurements of water and air, necessary for the calibration of the usual density measurement, allow the calculation of the ΔD_O values. The damping values that are obtained for the water calibration pertain to the first points of the calibration curve. Determining the ΔD_O values for any sample of known viscosity can be used to extend the range of the calibration curve.

Speed of Ultrasonic Pulses. The sound velocity, v, is measured by a pulse technique from the time it takes a short pulse with a center frequency of 3 MHz to pass through 5 mm of the sample.[6] A small correction for the delay time in the support can be determined by a water calibration measurement. This method is not designed to measure the sound dispersion or amplitude of the waves, but it is adjusted for high stability and easy use.

It is often more convenient to use only the relative difference of the sound velocity to that of the solvent, the so-called sound number s

$$s = \frac{v_{solution} - v_{solvent}}{v_{solvent}} \quad (7)$$

Combination of Density and Sound Velocity. Sound velocity and density are linked by means of the adiabatic compressibility β_S following the relation

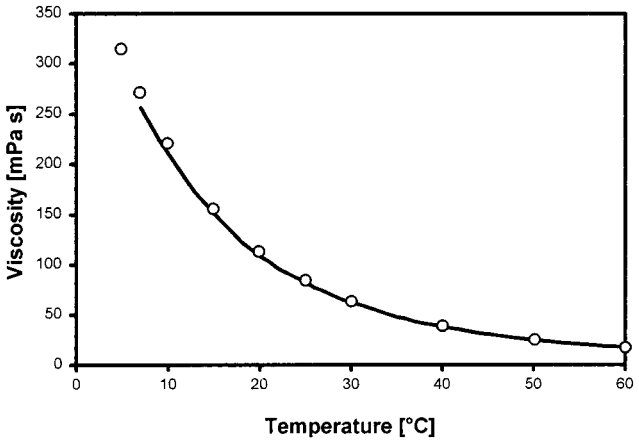

Figure 2. Viscosity of the density calibration silicon oil W46, measured with an Ubbelohde viscosimeter (○) and a DMA 5000 (solid line). The maximum viscosity, reliably accessible by means of the DMA, is about 270 mPa·s.

$$v = \sqrt{\frac{1}{\rho \cdot \beta_S}} \quad (8)$$

The isothermal compressibility, β_T, is a related value of great importance. To acquire it from the adiabatic compressibility, the formula

$$\beta_T = \frac{\beta_S c_P + \frac{T}{\rho^3} \cdot \left(\frac{d\rho}{dT}\right)^2}{c_P} \quad (9)$$

can be used, where T is the absolute temperature. The only parameter that is not accessible by means of the DMA is c_p, the heat capacity at constant pressure. Therefore, its value has to be taken from other sources.

Results

Ultralow Shear Viscosimetry. The quality of the viscosity data obtained by the DMA can be checked by means of silicon oils. Varying the temperature can give access to a wide range of different viscosities, while the viscoelastic contributions are kept small.

The deviations increase with increasing viscosity and reach about 5.6% at 271 mPa·s (Figure 2). The quality of the calculation is relatively high because this silicone oil shows nearly no viscoelastic behavior, whereas viscoelastic samples would give numbers that are too high.

For higher viscosities, the results would be too inaccurate due to the small change of the measured damping for rather important differences in viscosities. Therefore, these data points have been excluded by the evaluation software.

Isothermal Compressibility and Scattering of Water. The adiabatic compressibility of water can be obtained directly from the sound velocity and density data; the transformation into isothermal compressibility is straightforwardly accomplished with eq 9.

The results (Figure 3) are in good agreement with those found in the literature[19] and are of special interest for providing a complementary technique for small-angle scattering techniques because water is often used as a standard for calibration of the instruments to absolute intensity. The structure factor at zero scattering angle, $S(0)$, for monodisperse, homogeneous, uncharged spheres is related to the osmotic compressibility, β_{os}, of the particles.[20] However, for a pure substance, the osmotic

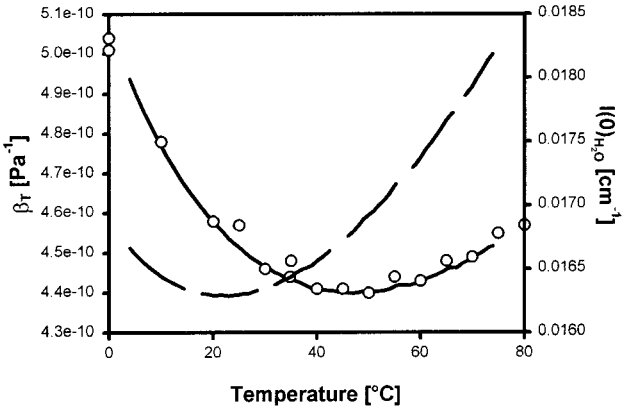

Figure 3. Isothermal compressibility, β_T, of water calculated from DMA data (solid line) compared to literature values from the CRC Handbook of Chemistry and Physics (○). The X-ray scattering intensity of water (dashed line) is calculated from the isothermal compressibility.

compressibility is equal to the isothermal compressibility, and the equation can be rewritten as

$$S(0) = nkT\beta_{os} = \frac{N_A\rho}{M_r}kT\beta_T \tag{10}$$

where N_A represents Avogradro and k the Boltzmann constant while M_r is the molecular mass and n the number of particles per unit volume. For a given type of radiation, the intensity in forward direction $I(0)$ can be calculated as[21]

$$I(0) = \frac{(\sum b_j)^2 S(0) N_A \rho}{M_r} \tag{11}$$

by using the scattering lengths of the atoms b_j.[22] Because of the small radius of a water molecule, the scattering intensity is nearly constant for the whole range of scattering angles that is usually measured for small-angle scattering experiments, giving a straight line with an intensity of $I(0)$.

Applications to Triblock Copolymers. The compressibility of water depends strongly on the local ordering of the molecules in the hydration layer around dissolved polymers or other molecules. This effect can be used for studying the formation of micelles; PEO−PPO−PEO triblock copolymers of the synperonic or pluronic type, such as P94, form micelles only above a certain critical temperature cmT,[23] which can be studied easily by performing density and sound velocity measurements at different temperatures.

The cmT can be detected by means of a drastic decrease in the solutions density because the density of the central PPO chain in the hydrophobic core is lower than in the hydrated form (Figure 4). The sound velocity depends, at least for small concentrations, on the amount of soluted substance. A considerable portion of its difference from water is due to the formation of a shell of differently structured water around the particles. This water shell has a different compressibility compared to the remaining solvent, leading to a change in the sound velocity.[24] However, during micelle formation, the number of soluted particles decreases, essentially leading to a reduced contribution of the water shell. By plotting the derivative of the sound number, the cmT can be seen as a broad peak (Figure 5). This effect cannot be explained as a consequence of the density change because, according to eq 8, the observed density change would lead to the opposite result, i.e., the increase of the compressibility affects the result much more than the decrease of the density.

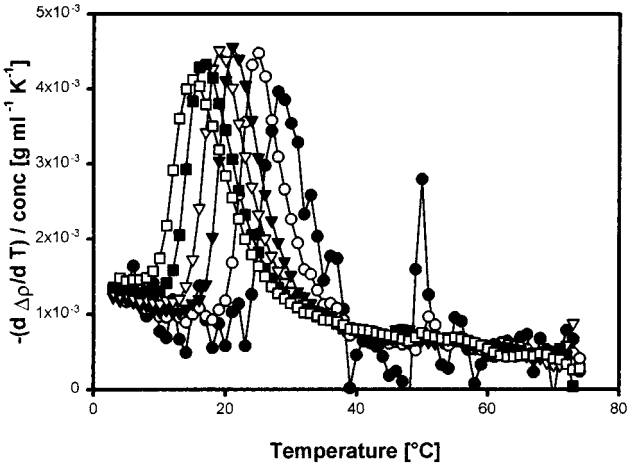

Figure 4. Negative derivative of the density difference between water and aqueous P94 solutions against temperature: 1% (w/w) (●), 5% (○), 10% (▼), 15% (▽), 20% (■), and 25% (□). The peak corresponds to micelle formation.

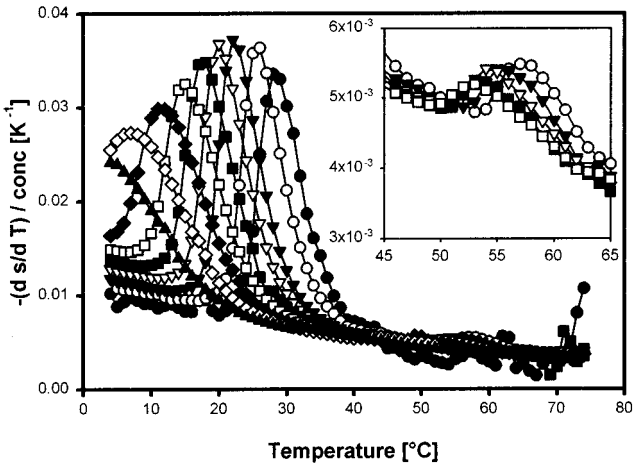

Figure 5. Negative derivative of the sound number of aqueous P94 solutions relative to water against temperature: 1% (w/w) (●), 5% (○), 10% (▼), 15% (▽), 20% (■), 25% (□), 30% (◆), 35% (◇), and 40% (▲). The main peak corresponds to micelle formation. The small peak around 60 °C (enlarged in insert) represents the formation of rodlike micelles.

A second, small but reproducible peak can be observed at higher temperatures (Figure 5). The structural change, which corresponds to this effect in the measured sound velocity, can be observed more easily by viscosimetry. Figure 6 shows that the reduced viscosity stays rather constant for all samples with less than 20% soluted P94 in the temperature regime from 3 °C to ∼54 °C. A rather drastic increase in viscosity can be observed at higher temperatures up to about 62 °C, at which another plateau value is reached. This rising viscosity can be attributed to the formation of elongated micelles that grow in length with increasing temperature.[25] The viscosity peak at about 30 °C, observed for P94 concentrations above 20%, is the first sign of gel formation at concentrations higher than 25.5%.

Concentrations higher than 25.5% show the formation of another sharp peak on top of the broad pregelling peak that can be attributed to the formation of a stiff gel. The measurement principle of the DMA prevents the correct evaluation of high viscosities or viscoelastic samples in terms of exact viscosity values, but the phase boundaries of the gel can be determined by means of the damping of the oscillator (Figure 7). The low damping signal at high viscosity (see also Figure 1) is the reason that some of the curves show values near zero for the gel, which

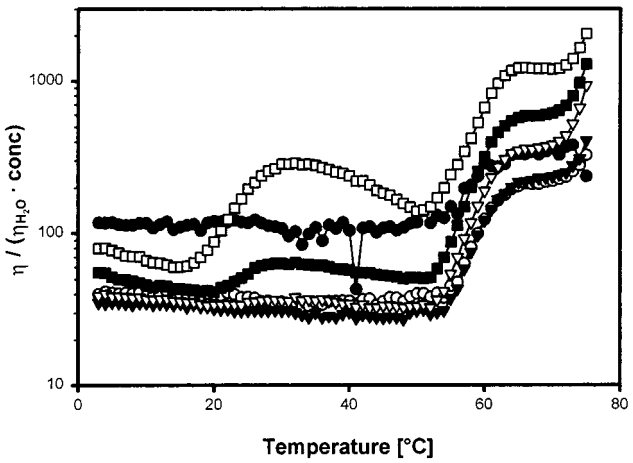

Figure 6. Reduced viscosities of aqueous P94 solutions divided by concentration: 1% (w/w) (●), 5% (○), 10% (▼), 15% (▽), 20%, (■) and 25% (□). The viscosity increase at 60 °C corresponds to the formation of rodlike micelles. The peak at 30 °C for 20% and 25% is a pregelling effect.

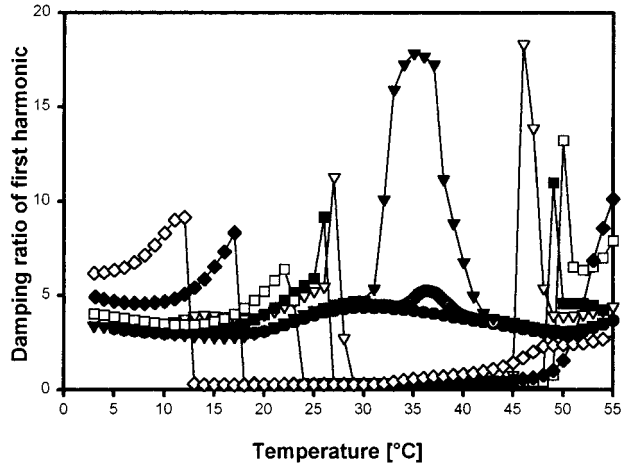

Figure 7. Gel formation of aqueous P94 solutions studied with the damping ratio of the oscillator: 25.5% (w/w) (●), 25.6% (○), 26% (▼), 27% (▽), 28% (■), 30% (□), 35% (◆), and 40% (◇). High damping values correspond to high viscosities. For viscosities much higher than 500 mPa·s, the damping collapses and a zero value is returned.

is extremely viscous, instead of high damping signals. The phase boundaries of the gel phase are given for these curves by the sharp edges, at which the signal changes abruptly.

A close look at the phase boundary between the micellar solution and the gel shows different behavior for heating than for cooling (Figure 8). A standard viscosity measurement, such as capillary rheology, leads to a difference in the transition temperature of 0.8 °C, whereas DMA measurements vary by 0.2 °C. Additional heating and cooling of the capillary rheometer gives different viscosities over about 2 °C, whereas the damping ratio measured by the DMA shows such a behavior only for a temperature range of 0.4 °C.

Application to Diblock Copolymers. Diblock copolymers of the C_iE_j type are nonionic surfactants and show, in aqueous solution, a critical temperature, T_c, above which demixing into a surfactant rich and a surfactant poor solution takes place (Table 1).[9]

Sound velocity measurements of such samples do not change significantly with increasing temperature up to T_c. The signal becomes more unstable above this temperature, but the variation is not very strong and sometimes hard to detect.

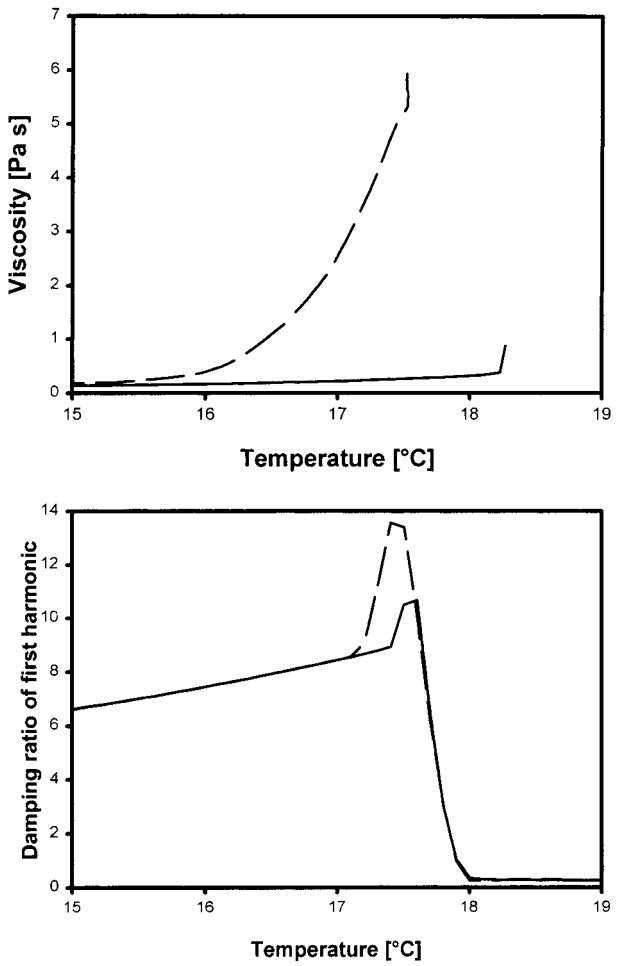

Figure 8. Shear-thinning effect of a 35% (w/w) P94 solution. (a, upper half) measured with a dynamic capillary rheometer at heating (solid) and at cooling (dashed) (b, lower half), measured with a DMA at heating (solid) and cooling (dashed).

TABLE 1: Critical Temperatures T_c of C_iE_j Solutions in D_2O at Critical Concentration Determined by DMA-viscosity Measurements, Visual Inspection and Compared to the Literature Values for C_iE_j in H_2O

surfactant	concentration (% (w/w))	T_c (DMA) (°C)	T_c (visual) (°C)	T_c (H_2O)[a,b] (°C)
$C_{12}E_6$	2.25	44.7	~45	51.3
$C_{12}E_5$	1.36	29.7	29.4	32.0
$C_{12}E_4$	0.90	3.2	3.4	6.6
$C_{10}E_4$	2.35	16.6	16.6	20.5
C_8E_5	8.75	57.5	55.6	61.7
C_8E_4	6.46	37.8	37.4	40.8
C_8E_3	4.72	6.0−6.4	6.0−6.3	11.0

[a] See reference 9. [b] Due to isotope effects the concentrations used by Schubert et al. are 2.5% ($C_{12}E_6$), 1.5% ($C_{12}E_5$), 1.0% ($C_{12}E_4$), 2.6% ($C_{10}E_4$), 9.6% (C_8E_5), 7.1% (C_8E_4) and 5.2% (C_8E_3).

The viscosities of such solutions increase with temperature (Figure 9), which can be attributed to the formation of of the sound number of aqueous P94 solutions relative to water micelles.[26] The nearly constant value that can be observed for the samples $C_{12}E_6$, C_8E_5 and C_8E_4 corresponds to spherical micelles existing at low temperatures. The reduced viscosity increases at higher temperatures because of a shape change from spheres to elongated particles, caused by the dehydration of the ethylenoxide chains. Most of the samples show a sudden change in the detected viscosity signal at high temperatures, which corresponds to the cloud point.[26] This is also proven by the almost complete lack of measurement points at even higher

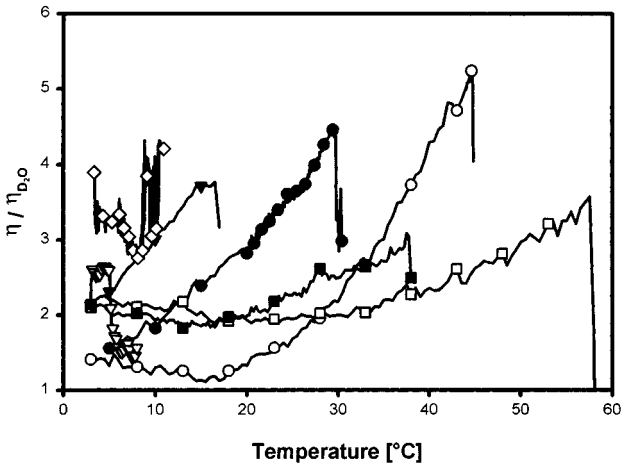

Figure 9. Reduced viscosities of C_iE_j solutions in D_2O at the critical concentrations: $C_{12}E_6$ (○), $C_{12}E_5$ (●), $C_{12}E_4$ (▽), $C_{10}E_4$ (▼), C_8E_5 (□), C_8E_4 (■), and C_8E_3 (◇).

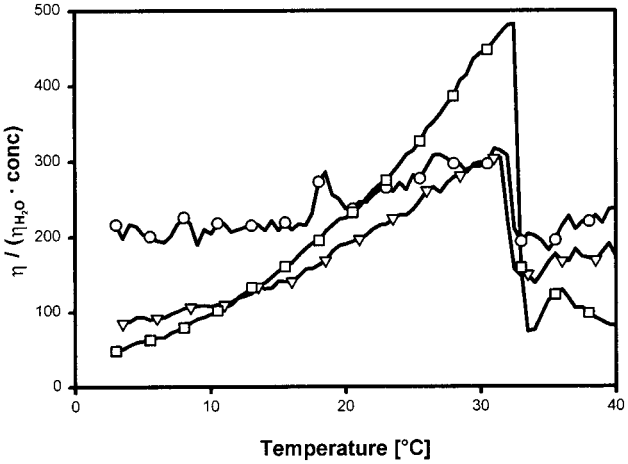

Figure 10. Viscosities of solutions of $C_{12}E_5$ in H_2O at the critical concentration of 1.5% (w/w) (▽), at 0.5% (○) and 4.5% (□).

temperatures because the DMA could not get a stable measurement signal in the two-phase region. The few points that could be obtained after the viscosity edge at the critical temperature demonstrate this intensely varying signal (Figure 9, $C_{12}E_5$ and C_8E_3). The critical temperatures of all of the samples observed in D_2O are some degrees below the values given for H_2O, as usual.

According to the phase diagrams of such C_iE_j surfactants, the cloud point reaches its lowest temperature at a fixed critical concentration. This can also be tested by means of the DMA, when measuring different concentrations (Figure 10). Besides the varying critical temperatures, the samples have a different relative viscosity increase with temperature, and the values change fastest for the samples with the highest concentration. The signals obtained from viscosity, density, and sound velocity measurements are not intense enough to extend the investigations to concentrations as low as the critical micelle concentration, cmc, of these nonionic surfactants.

Discussion

Ultralow Shear Viscosimetry: The viscosities obtained by means of the DMA have an error of less than 10%, but some limitations must be taken into account. The maximum in the damping signal sets an upper limit of about 300 mPa·s, whereas the lower limit is somewhere in the range of 0.5 mPa·s. A separation of G' and G'' is impossible, and the presence of elastic components alters the correct results. The impossibility of evaluating viscoelastic samples correctly is a major disadvantage of this measurement technique, but if the contribution due to elasticity is considerably less than the viscosity, such data can be evaluated like the purely viscous samples. Even for highly elastic samples, the qualitative temperature dependence can be studied by means of the damping data. A look at these data may even reveal whether the evaluation of some data points is impossible because of the high viscosity or because of the viscoelasticity. For example, the maximum damping value that can be achieved without viscoelasticity is in the range of 7.5 (Figure 1), whereas for viscoelastic samples, much higher damping values can sometimes be observed (e.g., Figure 6).

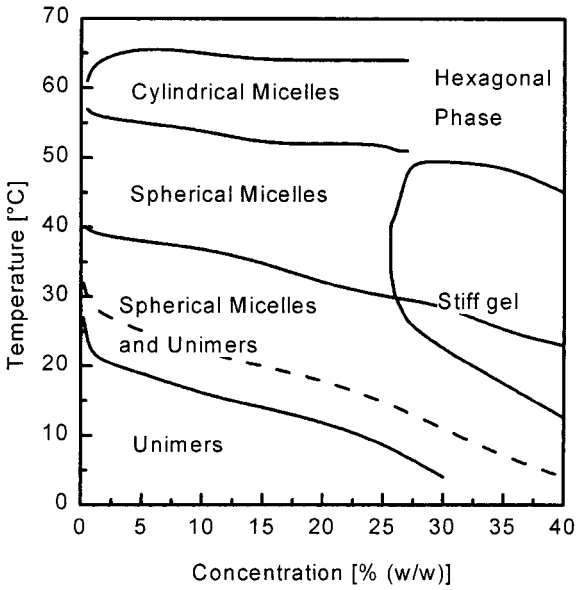

Figure 11. Phase diagram of aqueous P94, according to DMA results. The dashed line at low temperatures corresponds to the maximum building rate of spherical micelles. The solid lines next to this line represent the temperatures at which this micelle formation starts or finishes. The two solid lines at higher temperature show the limits of the temperature regime, at which cylindrical growth of the micelles takes place. There are some hints for phase boundaries at high concentrations and high temperatures, but the exact boundaries for the hexagonal phase must be determined by SAXS experiments.

Isothermal Compressibility and Scattering of Water. The compressibility measurements and calculations depend largely on the exact absolute values of the sound velocity and density. One great advantage in taking the DMA for such measurements is that all the necessary quantities that are used to calculate the isothermal compressibility and, consequently, the scattering intensity of the liquid, apart from the heat capacity, can be measured.

Applications to Triblock Copolymers. Phase diagrams of triblock copolymers usually differentiate only between the dilute isotropic L_1 phase and the dense phases, such as cubic, hexagonal, or lamellar. The techniques presented here allow us to distinguish between the existence of dissolved unimeres, globular micelles, and rodlike micelles within the L_1 phase. It is even possible to detect the course of micellization in detail, i.e., its onset, maximum formation rate with temperature, and temperature at which the micellization is completed. This results in much richer information in the phase diagram.

The data obtained for the different concentrations and temperatures of P94 allow the construction of a detailed phase diagram from 0.2% to 40% between 3 and 70 °C (Figure 11). The correct nature of the phases cannot be deduced directly from DMA data, but other techniques, such as SAXS and SANS,

are necessary.[2,28] Nevertheless, no contradiction remains between the observed changes in the DMA signals and the nature of the phases that are established by scattering methods. However, the transition temperatures can be detected much easier, faster, and more precisely by means of DMA data.

The peak in the derivative of the sound number, which corresponds to the formation of spherical micelles, has a width of nearly 20 °C. This is often attributed to the fact that P94 is an industrial product with a distribution of molecular masses and some impurities, such as diblock copolymers. The position and shape of the peak are in good agreement with the DSC results.[2]

The peak shifts to lower temperatures for higher concentrations, giving rise to an extremely broad concentration regime that corresponds to the cmc. It might be of special interest that the P94 phase diagram shows a region where micelle formation still takes place within the stiff gel, which has already formed at lower concentrations and temperatures.

Neither particle size nor size distribution can be determined by means of this ultrasonic speed cell, not only because of the inadequate wavelength but also because higher accuracy and more than one wavelength are necessary for such a calculation. Additionally, such an investigation is preferably accomplished with sound attenuation, not ultrasonic speed, because of the better signal.

The ultralow shear rates that are applied to the sample by the DMA reduce the shear-thinning effects to such a degree that only a small effect could be observed for the gel region. On the other hand, viscosity measurements, using a standard capillary rheometer, show massive shear-thinning effects, leading to highly different temperatures for the gel transition and viscosities, depending on the prior thermal history of the sample (Figure 8).

The structures at high temperatures, in the high concentration region, are not yet fully studied because of handling problems filling the DMA at low temperatures (below the gel region) without air bubbles, but SAXS experiments prove the existence of a hexagonal phase at these temperatures and concentrations.[28]

The overall features of the P94 phase diagram are comparable to other similar triblock copolymers. For example, the synperonic copolymer P85[2] shows the same formation of spherical micelles above a cmT, partially within the gel region. However, P85 has a higher percentage of ethylenoxide within the molecule, which keeps the molecules in solution better and consequently shifts the observed structures to higher temperatures (e.g., cylindrical micelles start to form at about 55 °C in P94 and 65° in P85). Another consequence of the increased amount of ethylenoxide is the growing space required for the micelles and the surrounding water. This results in the formation of the gel at concentrations about 23.5%, whereas the P94 gel forms above 25.5%.

Application to Diblock Copolymers. DMA viscosity measurements provide a fast and easy alternative to the usual time-consuming and tedious determination of the cloud point, by means of visual inspection. However, the cloud point can only be found by this technique if long, rodlike micelles are formed, which give the solution a high enough viscosity. On the other hand, viscosity itself can offer new information about the system, such as revealing another structural transformation between spherical and rodlike particles. Higher concentrations enhance this cylindrical growth because the slope is increased considerably.

Additionally, the good thermal control of the measurement cell allows the possibility of setting the correct temperature for the single-measurement points and consequently any sharp phase boundary, such as the critical temperature, with an accuracy of 10 mK. The ultralow shear rates applied by the oscillating tube are also of great importance for studying the samples near the critical temperature because high shear can affect the fluctuations, resulting viscosities, and phase transition temperatures.

Conclusion

The DMA offers an automatic, fast, and accurate method of establishing the phase diagrams of complex fluids with three independent parameters, which might detect a large variety of different phase boundaries and give first hints about the nature of the corresponding phases. It can detect micelle formation, sphere to rod transition, and demixing as a function of temperature or time, and it offers the absolute values for density, sound velocity, and viscosity. The ultralow shear, applied for viscosity measurements, is well suited for the study of tixotropic fluids.

Acknowledgment. This work was performed with project funding from the Austrian Fonds zur Förderung wissenschaftlicher Forschung, Grant No. P12611-CHE, and with the support of the Labor für Messtechnik, Graz and Anton Paar KG, Graz, Austria. We especially want to thank Hans Stabinger, Helmut Heimel, Klaus Ritzmann, and Ulrike Rakusch from the Labor für Messtechnik for their helpful discussions and practical assistance. We also want to thank Helga Katzer for performing the measurements with the capillary rheometer.

References and Notes

(1) Schillén, K.; Glatter, O.; Brown, W. *Prog. Colloid Polym. Sci.* **1993**, *93*, 66−71.
(2) Glatter, O.; Scherf, G.; Schillén, K.; Brown, W. *Macromolecules* **1994**, *27*, 6046−6054.
(3) Wen, X. G.; Verall, R. E. *J. Colloid Interface Sci.* **1997**, *196*, 215−223.
(4) Kratky, O.; Leopold, H.; Stabinger, H. *Z. Angew. Phys.* **1969**, *27*(*4*), 273−277.
(5) Orthaber, D.; Bergmann, A.; Glatter, O. *J. Appl. Crystallogr.*, **2000**, in press.
(6) Schneditz, D.; Kenner, Th.; Heimel, H.; Stabinger, H. *J. Acoust. Soc. Am.* **1989**, *86*(6), 2073−2080.
(7) Stabinger, H. *Proceedings of the Sheffield Meeting on Calibration, Calibration & Quality Standards in the 1990s*, Sheffield, 1994.
(8) Lehner, D.; Worning, P.; Fritz, G.; Øgendal, L.; Bauer, R.; Glatter, O. *J. Colloid Interface Sci.* **1999**, *213*, 445−456.
(9) Schubert, K.-V.; Strey, R.; Kahlweit, M. *J. Colloid Interface Sci*. **1991**, *141*, 21−29.
(10) Alexandridis, P.; Zhou D.; Khan, A. *Langmuir* **1996**, *12*, 2690−2700.
(11) Wanka, G.; Hoffmann, H.; Ulbricht, W. *Macromolecules* **1994**, *27*, 4145−4159.
(12) Mortensen, K.; Brown, W. *Macromolecules* **1993**, *26*, 4128−3135.
(13) Chu, B.; Zhou, Z. In *Nonionic Surfactants*; Nace, V. M., Ed.; Marcel Dekker Inc.: New York, 1996; Chapter 3.
(14) Stabinger, H.; Leopold, H.; Kratky, O. *Montash. Chem.* **1967**, *67*, 436−438.
(15) Kratky, O.; Leopold, H.; Stabinger, H. *Methods Enzymol.* **1973**, *27*, 98−110.
(16) Stabinger, H.; Sommer, K. D.; Fehlauer H. *ITG−Fachber.* **1995**, *126*, 549−554.
(17) Glatter, O. *J. Phys. IV* **1993**, *3*, 27−38.
(18) Leopold, H. *Telematik* **1995**, *1*(*2/3*), 12−18.
(19) McGowan, J. C. In *Handbook of Chemistry and Physics*, 73rd ed.; Lide, D. R., Ed.; CRC Press: Boca Raton, 1992; Chapter 6.
(20) Hansen, J. P.; McDonald, I. R. *Theory of simple liquids*; Academic Press: London, 1986.
(21) Klein, R.; D'Aguanno, B. In *Light Scattering, Principles and Development*; Brown, W., Ed.; Clarendon Press: Oxford, 1996; Chapter 2.
(22) Chen, S. H. *Annu. Rev. Phys. Chem*. **1986**, *37*, 351−399.
(23) Schillén, K. Solution Properties of Block Copolymers Studies Using Light Scattering. Dissertation, Uppsala 1994.

(24) Förster, F. Dielektrizitätskonstante und Schallgeschwindigkeit von Alkohol-Wasser-Gemischen. Dissertation, Göttingen, 1932.
(25) Lehner, D.; Lindner, H.; Glatter, O. *Langmuir* **2000**, *16*, 1689−1695.
(26) Glatter, O.; Fritz, G.; Lindner, H.; Brunner-Popela, J.; Mittelbach, R.; Strey, R.; Egelhaaf, S., submitted to *Langmuir*.
(27) Lang, P.; Glatter, O. *Langmuir* **1996**, *12*, 1193−1198.
(28) Bergmann, A.; Scherf, G.; Fritz, G.; Glatter, O., in preparation.